ELSEVIER

Thermochimica Acta 315 (1998) 159–168

thermochimica acta

# Temperature programmed decomposition of polypropylene: in situ FTIR coupled with mass spectroscopy study

Scott A. Hedrick, Steven S.C. Chuang*

*Department of Chemical Engineering, The University of Akron, Akron, OH 44325-3906, USA*

Received 19 September 1997; accepted 4 January 1998

**Abstract**

The temperature-programmed reaction (TPR) technique coupled with the in situ infrared (IR)/mass spectroscopy (MS) analysis has been employed to study the thermal decomposition of polypropylene. These techniques, especially when coupled with a gas chromatograph (GC), are effective for determining thermal stability, product distribution and product evolution as a function of temperature. The polymer decomposes at approximately 475 K yielding hydrocarbons in the $C_1$–$C_7$ range, with propylene, $C_5$ and $C_6$ composing the majority of gaseous products. Decomposition over alumina and 5 wt% $Ni/Al_2O_3$ with and without the presence of hydrogen does not affect thermal stability. Also, decomposition over alumina with and without the presence of hydrogen does not affect the depolymerization pathway. The popular β-scission/backbiting mechanism cannot fully explain observations from this study. Possible alternatives are explored. © 1998 Elsevier Science B.V.

*Keywords:* Polypropylene; Polymer decomposition; Depolymerization; Temperature-programmed reaction; Chemical recycling

## 1. Introduction

The development of viable recycling technologies for plastic waste materials is becoming increasingly important as landfill space shrinks. One possible solution, a plastics-to-chemicals recycling process, holds particular promise. However, the development of useful and economical chemical recycling technology necessitates the ability to evaluate and understand the thermal stability of recyclable thermoplastic polymers and the decomposition pathway under various process conditions. The evaluation method we have recently developed is the simultaneous use of Fourier transform infrared spectroscopy (FTIR) and mass spectrometry (MS) for the in situ infrared and temperature-programmed reaction (TPR) studies of plastics. In this study, polypropylene (PP) will serve as the subject of evaluation. This approach will allow the simultaneous evaluation of bond breaking and product formation during polymer decomposition. There have been numerous studies in the past which investigated various aspects of depolymerization [1–16]. These studies describe a wide range of experiments with varying techniques and conditions that examine decomposition of a number of different thermoplastics. All these studies tend to focus on the final product distribution after the completed reaction and do not monitor the reaction as it is taking place. No study was found which uses simultaneous in situ FTIR/MS for the evaluation of polymer decomposition.

*Corresponding author. Fax: 00 1 216 972 5856; e-mail: schuang@uakron.edu


*PII* S0040-6031(98)00283-4

The first objective of this work was to demonstrate the usefulness of simultaneous operation of MS/FTIR for the in situ TPR of polypropylene to study the thermal stability, product formation and decomposition pathway. The second objective was to elaborate upon the advantages and limitations of this technique. This type of study may lead to technological improvements in chemical recycling, including improvements in catalyst and process design.

## 2. Experimental

### 2.1. Polypropylene sample preparation

Two forms of polypropylene were used in this study – powder and film. Polypropylene powder (manufactured by Monteil polyolefins) was used for the experiments involving a tubular reactor. Polypropylene film was used for transmission FTIR and diffuse reflectance infrared Fourier transform spectroscopy (DRIFTS) studies. In order to produce a thin polypropylene film, the powder was dissolved in toluene at a proportion of 0.2 g/15 $cm^3$. While being careful not to bring the polypropylene solution to a boil, it was heated slowly until all the toluene was evaporated. If the toluene was boiled away, bubbles would become trapped in the polypropylene film, ruining the sample for infrared analysis. Evaporation of the toluene led to precipitation of a thin film at the bottom of the beaker.

### 2.2. Catalyst preparation

A 5 wt% $Ni/Al_2O_3$ catalyst was prepared by the impregnation of γ-α aluminum oxide (Alfa Aesar, 100 $m^2$/g, purity: 99.98%) using nickel (II) nitrate hexahydrate ($Ni(NO_3)_2 \cdot 6H_2O$) solution. The ratio of the solution to the weight of support material was approximately 1.5 $cm^3$ to 1 g. The catalyst was dried over a period of two days in air at room temperature after impregnation. Finally, the catalyst was calcined for 3 h under 25 $cm^3$/min air flow and then reduced for 16 h under 15 $cm^3$/min hydrogen flow, both at 673 K.

### 2.3. Temperature-programmed reaction (TPR) studies

The initial TPR experiments were conducted in a 3/8″ o.d., 1/4″ i.d. stainless steel tubular reactor. Helium flow at 50 $cm^3$/min served as the carrier gas. This and all subsequent experiments followed the same heating history in which the reactor was heated from 293 to 673 K at a rate of 10 K/min. The temperature was then held constant for 30 min at 673 K and then allowed to cool back down again at the rate of 10 K/min. The effluent was monitored by MS/FTIR/GC. The MS utilized was a Balzers QMG 112 quadrupole with an axial secondary electron multiplier, capable of the simultaneous monitoring of eight m/e ratios. The IR spectra, with use of a gas sampling cell [17], were recorded by a Nicolet 5SCX FTIR spectro-

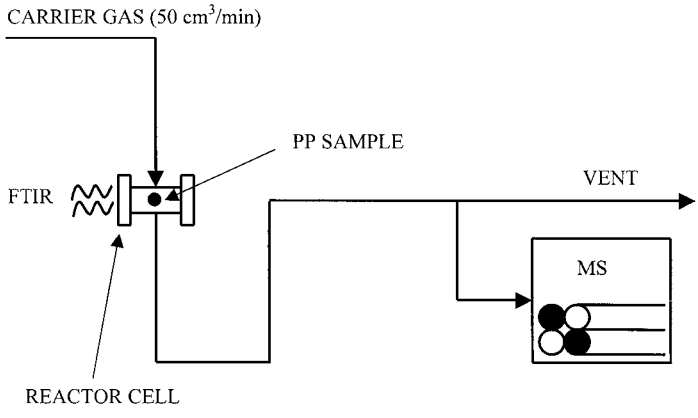


Fig. 1. Flow system for the in situ TPR.

meter with a DTGS detector at 4 $cm^{-1}$ resolution. Gaseous effluent samples with a volume of 1 $cm^3$ were pulsed into a Hewlett-Packard 5890 gas chromatograph (GC) with Porapak PS and QS columns in series and flame-ionization detector (FID) at what was determined to be the point of maximum product production during TPR, approximately 553 K.

Although the tubular reactor allows the use of large sample sizes, it does not allow for the in situ FTIR monitoring of the depolymerization process. For the in situ monitoring, both transmission IR and DRIFTS were utilized. These in situ IR–TPR techniques are illustrated in Fig. 1. For the transmission IR, the polypropylene sample disks were sandwiched between two self-supporting alumina disks and placed in the center of the reactor [18] with the tip of a thermocouple touching near the center for accurate temperature measurement. For the DRIFTS, either powder or film polypropylene were mixed with either 5 wt% $Ni/Al_2O_3$ or $Al_2O_3$ and placed in the cylindrical holding tray. Both helium and 10 percent hydrogen in helium served as the carrier gas during TPR. The DRIFTS spectra were recorded by a Nicolet 550 Magna FTIR spectrometer with an MCT-B detector.

### 2.4. MS calibration

The MS analog scan, which monitors m/e ratios from 1 to 200 approximately every minute, was employed to determine all the m/e ratios resulting from the decomposition. The resultant spectra suggested a number of possible products ranging from $C_1$–$C_7$. In order to determine the contribution of each product to a given m/e peak and better determine the

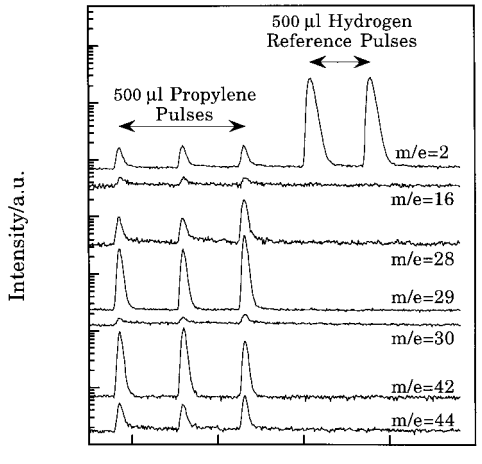


Normalization procedure for obtaining m/e intensity values:

1. Let $A_i$=avg. area under the i fragment response pulses
2. Pick an m/e ratio as a basis and assign it an intensity value--$I_b$*
3. Let $I_i=I_b[A_i/A_b]$, where $I_i$=intensity value of fragment i and $A_b$=avg. area under the basis fragment response pulses

| Propylene | |
|---|---|
| m/e ratio | $I_i$ |
| 44 | 13.88 |
| 42 | 69.00 |
| 30 | 1.32 |
| 29 | 40.73 |
| 28 | 52.92 |
| 16 | 2.76 |
| 2 | 43.06 |

Fig. 2. Calculation procedure for obtaining the relative peak values from MS calibration pulses using propylene as an example. (*) This value was taken from literature [19].

parent gaseous products, it was necessary to examine the fractionation patterns of a number of likely low-molecular weight depolymerization products, including methane, ethane, ethylene, propane, propylene, *n*-pentane, hexane and heptane. The gas samples – methane, ethane, ethylene, propane and propylene, were pulsed into the MS, entering the carrier gas through a 6-port sampling valve with a 500 μl sampling loop. Fig. 2 shows the response of three propylene pulses followed by two hydrogen pulses, which were used as a reference for the comparison of different calibration species. The propylene pulses produced fragmentation at m/e=2, 16, 28, 29, 30, 42 and 44. The liquid samples – pentane, hexane and heptane, 1 μl in size, were injected into the carrier gas with a syringe through a septum. The stainless steel tubing leading to the MS was heated to 383 K to ensure that the entire sample entered the MS in the gas phase.

## 3. Results

Fig. 3 shows the selected m/e profiles of products for the TPR of polypropylene in the tubular reactor. The repeated run indicated reproducibility in that the product formation began at the same temperature and

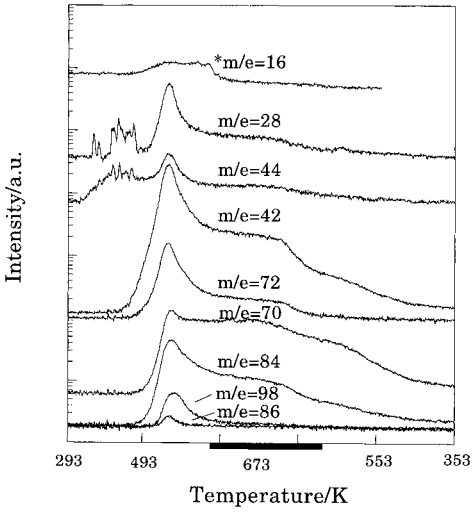


Fig. 3. TPR product response for PP decomposition in tubular reactor amidst 50 cc/min. He flow. PP sample=585.6 mg. Heavy dark line indicates the range of constant temperature. (*) Response curve was taken from repeated run.

the shared m/e peaks exhibited the same qualitative form. The peak at m/e=16 from the repeated run is included in Fig. 3. The m/e=28 and m/e=44 curves, because of a flow disturbance, experienced some initial interference. Normalization of the MS response curves by $E(t) = C(t)/\int_0^\infty C(t)\mathrm{d}t$, where $C(t)$ is the response curve and $E(t)$ is the normalization curve, was performed so that all m/e profiles would have an area equal to one under the curve, allowing for a fair comparison of the lead/lag relationships. It was found that all products began forming between 475 and 485 K, with the higher molecular weight species at m/e=70, 72, 84, 86 and 98 lagging slightly behind.

To quantify the product distribution, 1 $cm^3$ samples were taken for GC analysis at the point of maximum product production, approximately 553 K. Results are summarized in Table 1. It was difficult to separate olefin from paraffin products for hydrocarbons greater than or equal to $C_5$ with the Porapak PS and QS columns; thus, they are simply labeled as $C_5$, $C_6$ and $C_7$. In order to estimate mole percents for these species, an average calibrating factor, accounting for olefins and paraffins, was used.

Precise quantification of the MS results is impossible due to the large degree of m/e overlap; however, with the combined GC and MS calibration results, an attempt has been made to determine which species contribute to each respective response curve. A summary of these assignments and accompanying rationale are shown in Table 2.

Fig. 4, representing the corresponding IR data of the gaseous effluent of the tubular TPR, shows several prominent peaks, including 2968, 1661, 1465 and 1381 $cm^{-1}$, representing $CH/CH_2/CH_3$ stretching, C=C stretching, asymmetric $CH_3$ bending and sym-

Table 1
GC product quantification at 553 K for TPR in tubular reactor

| Species | Exp.1 (176.6 mg PP) | | Exp.2 (585.6 mg PP) | |
|---|---|---|---|---|
| | Mol% | Wt% | Mol% | Wt% |
| Methane | 5.8 | 1.7 | 3.8 | 1.0 |
| Ethane | 8.7 | 4.8 | 5.7 | 2.7 |
| Ethylene | 1.5 | 0.8 | 0.5 | 0.2 |
| Propylene | 37.6 | 29.3 | 22.9 | 15.3 |
| Butene | 5.8 | 6.0 | 2.4 | 2.1 |
| $C_5$ | 26.0 | 34.3 | 39.0 | 44.0 |
| $C_6$ | 14.5 | 22.8 | 25.8 | 34.8 |
| $C_7$ | 0.2 | 0.3 | – | – |

Table 2
MS m/e peak assignments

| m/e | Possible species | Rationale |
|---|---|---|
| 98 | Heptene | Heptene is the only species within range that would give a 98 peak. |
| 86 | Hexane | Hexane is the only species within range that would give an 86 peak. |
| 84 | Hexene | Although hexane also gives an 84 peak, 84 ($I_i$=1.92) and 86 ($I_i$=8.75) do not follow the same pattern. |
| 72 | Pentane | Pentane is the only species that gives a 72 peak. |
| 70 | Pentene | No hydrocarbons from the calibration yield a 70 peak; thus, it is most likely from pentene fragmentation. |
| 58 | Butene | Cannot be butane – none found in GC. Most likely butene |
| 44 | Propylene, $C_5$, $C_6$ | Cannot be propane – none found in GC. Mostly propylene with small $C_5$/$C_6$ contribution. |
| 42 | Propylene, $C_5$, $C_6$ | All these possible species give 42 peaks and are found in GC. |
| 30 | Ethane | Only species with a substantial 30 peak. |
| 28 | Ethane, ethylene, propylene, hexane | All these possible species give 28 peaks and are found in GC. |
| 16 | Methane | Only species with a substantial 16 peak. |

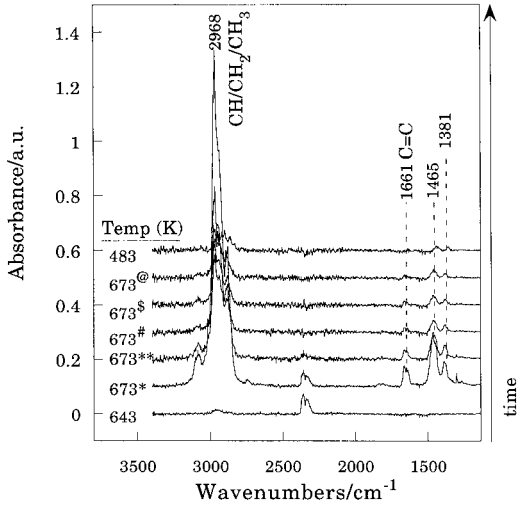


Fig. 4. Infrared spectra of gaseous effluent from PP decomposition in tubular reactor amidst 50 cc/min He flow. (*) After 7 min; (**) after 11 min; (#) after 17 min; ($) after 20 min; (@) after 29 min.

Table 3
Prominent IR band assignment

| Wavenumbers | Assignment |
|---|---|
| 808 | C–C s, $CH_2$ r |
| 837 | C–H r |
| 895 | $CH_3$ r, C–C s |
| 973 | $CH_3$ r + C–C s |
| 997 | $CH_3$ r |
| 1163 | C–C s + C–H w –$CH_3$ r |
| 1372–1381 | $CH_3$ sb |
| 1453–1465 | $CH_3$ ab |
| 1661 | C=C s |
| 2858–2972 | $CH_2$/$CH_3$ as, CH/$CH_2$/$CH_3$ s |

ab=asymmetrical bending.
as=asymmetrical stretching.
r=rocking.
s=stretching.
sb=symmetrical bending.w=wagging

metric $CH_3$ bending, respectively. A summary of pertinent IR band assignments as found in literature [20,21] is shown in Table 3. It should be noted that the CH, $CH_2$ and $CH_3$ symmetric stretching bands as well as $CH_2$ and $CH_3$ asymmetric stretching bands are all overlapped between 2900 and 3000 $cm^{-1}$. The peak in this region will be referred to as the CH/$CH_2$/$CH_3$ stretching region. The delay in appearance of the IR bands with respect to the MS bands can be attributed to the time necessary to travel from the MS to the FTIR spectrometer. The characteristic gas-phase $CO_2$ peaks at 2362 and 2337 $cm^{-1}$ are attributable to the flow fluctuations found within an air vent inside the IR sampling chamber and in no way represent the polymer decomposition. The C=C stretching band is unique for olefins while the CH/$CH_2$/$CH_3$ stretching bands exist for both olefins and paraffins. From the Aldrich Library of FT-IR spectra [22], it can be assumed that for pure $C_5$ and $C_6$ olefins, the ratio of the 2968 $cm^{-1}$ band (CH/$CH_2$/$CH_3$ stretching) height to the 1661 $cm^{-1}$ band (C=C stretching) height is approximately 3.75 : 1 while that for propylene is

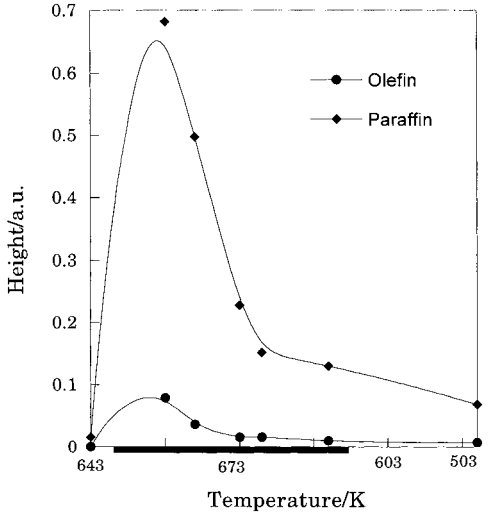


Fig. 5. Olefin/paraffin response curves derived from IR data taken of gaseous effluent from tubular reactor.

about 2 : 1. Thus, to estimate the olefinic and paraffinic contributions to this peak, 3.75 times the height of the 1661 $cm^{-1}$ peak was subtracted from the height of the 2968 $cm^{-1}$ peak. The resultant peak height represents the paraffin contribution to the 2968 $cm^{-1}$ peak and, along with the 1661 $cm^{-1}$ peak height for olefins, is plotted in Fig. 5 versus temperature, giving a qualitative estimate of the amounts of each present in the effluent as a function of temperature. The fact that the propylene ratio is not accounted for in the calculation indicates that this is a conservative calculation.

In order to compare the GC results with literature, it was necessary to convert mole percents to weight percents. In the case of $C_5$ and $C_6$ products, the average molecular weights were used, i.e. 71 for $C_5$ and 85 for $C_6$. On a mole percent basis, propylene, $C_5$ and $C_6$ accounted for the majority of products, from 78.1% (86.4 wt%) in the first run to 87.7% (94.1 wt%) in the second. Although variation in mole percents differed between the runs, the relative product distributions are quite similar and qualitatively match the MS results. A number of studies report product distributions in the form of weight percents for polypropylene decomposition over various catalysts with widely varying results. Decomposition over ZSM-5 catalyst in a steady flow system with helium as the carrier gas produced $C_4/C_5$ species as the gaseous products with the highest weight percent at 42.44%, followed by propane and methane at 27.84% and 16.90%, respectively [4]. For decomposition over DEZ catalyst, the top three hydrocarbons produced were methane, propylene and propane at 42.68 wt%, 21.46 wt% and 9.54 wt%, respectively. The product distribution for polypropylene decomposition over H-ZSM-5 catalyst in an evacuated batch reactor at 623 K has also been reported [11]. Of the 74 wt% of the products that can be classified as volatile or gaseous, $C_3$ was produced the most at 37.0 wt% followed by $C_4$ and $C_5$ at 15.3 wt% and 5.8 wt%, respectively. Also, they report 5.9 wt% aromatics. There appears to be little consistency in product distribution, probably due to the differences in reaction conditions as much as differences in catalysts. Interestingly, our results would indicate that no propane is being formed nor is there any evidence of the formation of aromatics. Most of the m/e=44 peak from Fig. 3 can be attributed to propylene. From the calibration results, propylene does give a significant peak at m/e=44; this relatively common phenomenon is explained in the literature as 'hydrogen abstraction' – abstraction of an hydrogen atom from another species by the molecular ion [23,24]. Although it appears that H-ZSM-5, ZSM-5 and DEZ exhibit catalytic activities, they do not provide definite advantages in selectivity over simple thermal decomposition of polypropylene nor is it clear exactly how these catalysts act mechanistically to alter product distribution. In other words, in no instance is there a specific product whose relative production is overwhelming.

Fig. 6 shows the MS data corresponding to the transmission IR experiment, decomposition on alumina amidst He flow. Product formation began around 490 K. Normalizing the peaks and comparing them to the tubular TPR MS results, it is again apparent that the higher molecular weight species, $C_5$, $C_6$ and $C_7$, lag $C_1$, $C_2$, $C_3$ and $C_4$. The run was repeated with hydrogen composing 10 percent of the carrier stream. The resultant MS hydrocarbon profiles from this run are nearly identical to the original 100% helium run with respect to the peak size and time of appearance, suggesting that hydrogen plays no role in the thermal stability or cracking mechanism. Also, because these results follow closely those of the tubular reactor, the presence of alumina appears not to have a catalytic effect.

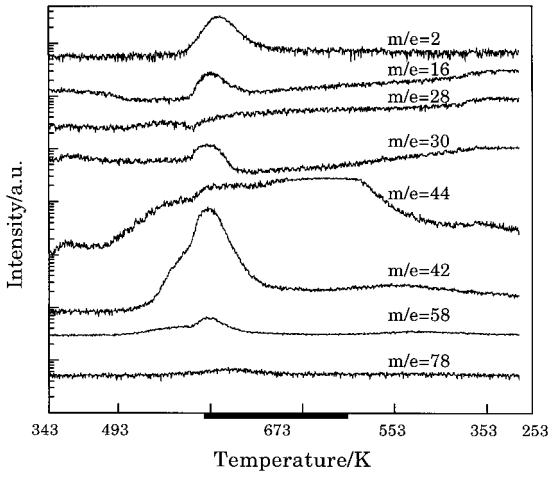


Fig. 6. TPR product response for PP decomposition on $Al_2O_3$ amidst 50 cc/min He flow, low-temperature reactor. PP sample=32.5 mg.

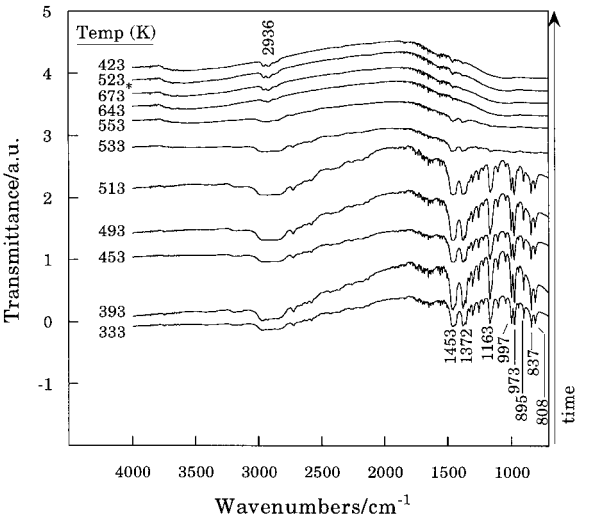


Fig. 7. Infrared spectra of PP decomposition on 5 wt% $Ni/Al_2O_3$ amidst 50 cc/min 9 : 1 He : $H_2$ flow, DRIFT. PP sample=5.0 mg. (*)After 20 min.

The transmission IR data corresponding to these MS results shows that the only visible bands, asymmetric $CH_3$ bending and symmetric $CH_3$ bending, located at 1458 and 1376 $cm^{-1}$, respectively, disappear simultaneously. The $CaF_2$ windows in conjunction with the alumina disks cause a limited range of transmission, from 1200 $cm^{-1}$ to around 2600 $cm^{-1}$.

From the IR results alone, it is difficult to determine at what point the polymer decomposes. However, the MS results provide a conclusive insight into the thermal stability. The MS results indicate that initial decomposition occurs between 450 and 490 K whether hydrogen is present or not. Interestingly, this is not much beyond the melting point of polypropylene, 443 K, indicating that 450 K is probably slightly in error. On the other hand, the 490 K figure obtained from the transmission experiment is reproduced, suggesting that this number is closer to the actual point of initial decomposition. Other studies [4,5,11] perform polypropylene decomposition under conditions ranging from 623–843 K, but none report information regarding the threshold of stability or the transient nature of the reaction.

The use of the DRIFTS apparatus, as Fig. 7 demonstrates, provides far superior spectra than the transmission spectra. All the prominent characteristic polypropylene bands can be clearly discerned. With the use of these clear spectra, it was desirable to examine how the bonding changes within the polypropylene as the reaction takes place. As the temperature was increased, all bands decreased in the same way, disappearing simultaneously. The polymer bands began receding after 493 K and disappear completely by 643 K, with the most rapid decrease in intensity between 513 and 533 K. Because the decomposition occurs very rapidly, the time resolution does not allow the clear determination of the bond breaking/bond forming sequence. It is impossible to discern which bonds – C–C bonds, C–H bonds, or C–$CH_3$ bonds – are being broken first or broken at all. It is also impossible to discern which product bonds are formed first as well. The decomposition of polypropylene results in a large number of products, all of which contain the same hydrocarbon bonding, which again is very similar to the bonding that exists within polypropylene. Fortunately, information concerning thermal stability can still be retrieved.

Repeated runs without $Ni/Al_2O_3$ present provided identical results, suggesting that the presence of $Ni/Al_2O_3$ does not affect the thermal stability. The remaining $CH/CH_2/CH_3$ stretching band at 2936 $cm^{-1}$ probably can be attributed to the adsorbed gaseous product. This band is prominent in poly-

propylene as well as in low-molecular weight hydrocarbons. The MS results for the set of DRIFTS runs was unable to provide additional insight into the observed IR phenomena. Because of the extremely small sample size, the gaseous products were not at a concentration high enough to be detected.

Simultaneous MS/IR measurement of polypropylene TPR allows the in situ monitoring of the reaction process and any anomalous behavior of the reaction system. For example, the behavior of the m/e=28 and m/e=44 curves from Fig. 6 was probably caused by a small leak in the reactor. The presence of nitrogen caused the initial m/e=28 baseline to be over an order of magnitude higher than that of the tubular runs, thus overwhelming any response by decomposition products.

## 4. Discussion

Because of the reproducibility of results between the experimental runs, we can conclude with reasonable confidence that the presence of hydrogen and alumina do not affect the thermal stability, the pathway of decomposition, nor product distribution. Although $Ni/Al_2O_3$ does not appear to affect the thermal stability, it cannot be stated conclusively that it does not affect the pathway or product distribution due to the lack of MS results for the DRIFTS runs.

One commonly proposed pathway for polypropylene decomposition is described below [5,25,26]:

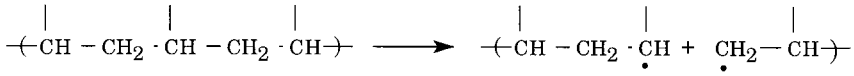
(1)

Step 1. A random C–C scission forms a primary and secondary carbon radical:

Step 2. An intramolecular radical transfer, or backbiting, takes place in which tertiary radicals are formed from the less stable primary and secondary radicals:

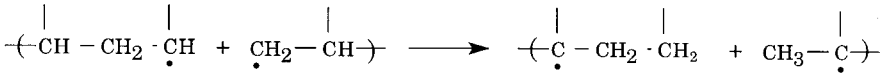
(2)

These tertiary radicals do not necessarily have to exist at the appropriate carbon closest to the chain end.

Step 3. β-scission, a process by which the tertiary radical decomposes to form a 1-olefin and another radical, occurs. For instance, the products from step 2 are shown below undergoing β-scission to form $C_4$ and $C_6$ alkenes.

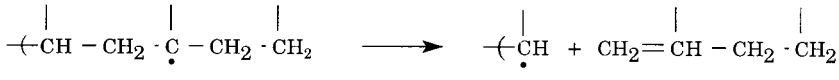
(3)

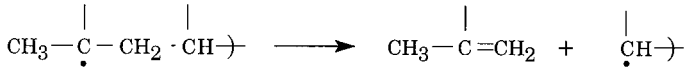
(4)

Step 4. In addition to undergoing backbiting and β-scission, radicals can undergo intermolecular reactions by gaining a hydrogen ($+H^{\bullet}$) to form a paraffin or by losing a hydrogen atom ($+H^{\bullet}$) to form an olefin:

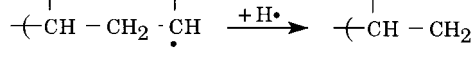
(5)

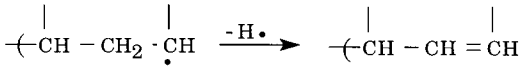

(6)

The results obtained from our study indicate that the backbiting/β-scission mechanism probably is not a major pathway for our polypropylene decomposition. First of all, β-scission, if occurring on chains where the tertiary radical is located on the closest possible carbon to the chain end as shown is step 2, would yield exclusively $C_4$ and $C_6$ olefins. Although the results of this study indicate a sizable $C_6$ fraction, the butene fraction was not higher than 5.8 mol%. Also, the backbiting/β-scission mechanism cannot account for the large presence of propylene and $C_5$ hydrocarbons.

Propylene can be formed if β-scission occurs without backbiting. This is shown below for a secondary carbon radical produced by step 1.

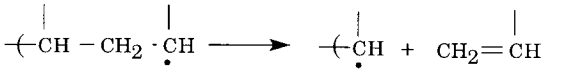

(7)

Formation of propylene from a primary radical is also possible:

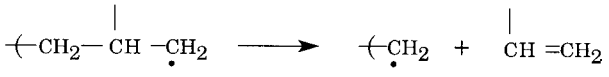

(8)

One possible mechanism for the production of $C_5$ products can be explained by scissioning between carbon 3 and carbon 4 as shown below:

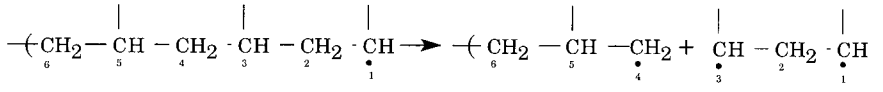

(9)

(10)

The first reaction given above would most likely produce an olefin while the second reaction could form a paraffin by gaining a hydrogen or an olefin by losing a hydrogen as outlined in step 4. The formation of $C_6$ can also be explained by this mechanism if scissioning occurs between carbons 4 and 5.

An alternative mechanism for the formation of $C_5$ and $C_6$ hydrocarbons could occur if the products from step 1 underwent isomerization to form secondary radicals as shown below:

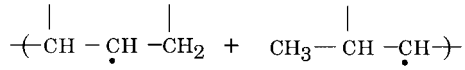

A subsequent β-scission would yield $C_5$ for the left-hand species and $C_6$ for the right-hand species.

Herman Pines, in his discussion of hexadecane cracking mechanisms, lends support to the feasibility of this mechanistic scheme [27]. There are instances in Pines' mechanism in which secondary carbocations are formed from tertiary carbocations through an intramolecular rearrangement prior to product formation via β-scission. Although his discussion centers around carbocations, the extension to radicals could easily be made since the stability of radicals and carbocations follow the same trend.

The overall mechanistic scheme, as shown in steps 1–4, would most likely yield a preponderance of olefins, which can be formed in step 3 and step 4, while paraffins can only be formed by step 4. According to the previously discussed IR results shown in Fig. 5, the majority of the product can be classified as paraffins. This, along with the fact that the formation of $C_4$ precedes the formation of $C_6$, suggests that backbiting/β-scission is not occurring to a great extent, since this would lead to the simultaneous production of both $C_4$ and $C_6$ hydrocarbons. The product distributions obtained in this study can be accounted for only if the decomposition precursors exist as primary and secondary radicals or, in other words, if the formation of the majority of products bypasses the backbiting step.

## 5. Conclusions

The results suggest that, in general, $C_1$–$C_4$ hydrocarbons appear followed by $C_5$/$C_6$ and then by $C_7$,

with initial decomposition occurring around 480 K. The $C_5/C_6$ hydrocarbons account for an average of 52.7 mol% of the product. Propylene by itself averages 30.3 mol% while the combined contribution of $C_1$, $C_2$ and $C_4$ accounts for 17.0 mol%. The $C_7$ contribution is barely a trace. In addition, this study was able to determine that $Al_2O_3$ and 5 wt% $Ni/Al_2O_3$ with and without the presence of hydrogen had no apparent effect on thermal stability and that neither $Al_2O_3$ nor hydrogen noticeably changed the decomposition pathway/product distribution. In other words, the catalyst active sites are not accessible to polypropylene for catalytic cracking.

The backbiting/β-scission mechanism does not appear to be the major pathway by which the polypropylene TPR in this study followed. This scheme cannot account for the product distribution nor the lead/lag product relationships observed in this study. The products are most likely being formed (a) by β-scission of the radicals without backbiting occurring first and (b) scissioning occurring near the chain ends followed by the loss or gain of a hydrogen atom. In other words, the product distribution from this study can only be accounted for if there is little intramolecular radical transfer prior to scissioning.

These experimental techniques are effective for determining the thermal stability, product distribution and product evolution as a function of temperature. However, an IR with better time resolution is needed for the elucidation of additional mechanistic information. The future utilization of a new 64-channel MS in conjunction with a 16-port sampling valve for multiple GC data points should clarify any ambiguity in MS peak assignments/product distribution.

## References

[1] M. Bellahcene, N. Bounafa, ANTEC (1991) 720.
[2] H. Ohkita, R. Nishiyama, Y. Tochihara, T. Mizushima, N. Kakuta, Y. Morioka, A. Ueno, Y. Namiki, S. Tanifuji, H. Katoh, H. Sunazuka, R. Nakayama, T. Kuoyanag, Ind. Eng. Chem. Res. 32 (1993) 3112.
[3] Z. Zhang, T. Hirose, S. Nishio, Y. Morioka, N. Azuma, A. Ueno, Ind. Eng. Chem. Res. 34 (1995) 4514.
[4] C. Vasile, M. Sabliovschi, V. Barboiu, Revue Roumaine de Chimie 40(7)–8 (1995) 679.
[5] R.P. Lattimer, Journal of Analytical and Applied Pyrolysis 31 (1995) 203.
[6] W. Kaminsky, B. Schlesselmann, C. Simon, Journal of Analytical and Applied Pyrolysis 32 (1995) 19.
[7] Z. Shen, M. Day, D. Cooney, Recycling II (1993) 449.
[8] J. Bonilla-Rios, R. Darby, J.M. Sosa, ANTEC (1995) 1630.
[9] A. Larena, M.U. De La Orden, J.M. Urreaga, Polym. Degrad. Stab. 36 (1992) 81.
[10] D.V.J. Lacoste, G. Dauphin, Polym. Degrad. Stab. 45(3) (1994) 355.
[11] R.C. Mordi, J. Dwyer, R. Fields, Polym. Degrad. Stab. 46(1) (1994) 57.
[12] A. Onishi, S. Uchino, N. Oguri, X. Jin, Anal. Sci. 10 (1994) 271.
[13] M.J. Brues, M.R. Kamal, D.G. Cooper, ANTEC (1995) 3720.
[14] C.Q. Yang, L.K. Martin, J. Appl. Polym. Sci. 51(3) (1994) 389.
[15] A.B. Bjerre, E. Sorenson, Ind. Eng. Chem. Res. 33 (1994) 736.
[16] E. Borsig, A. Fiedlerova, L. Hrckova, Pure Appl. Chem. A32(12) (1995) 2017.
[17] S.S.C. Chuang, M. Brundage, M. Balakos, G. Srinivas, Appl. Spec. 49 (1995) 1151.
[18] S.S.C. Chuang, S.I. Pien, J. Catal. 135 (1992) 618.
[19] F.W. McLafferty, D.B. Stauffer, The Wiley/NBS Registry of Mass Spectral Data, Vol. 1, Wiley, New York, 1989.
[20] D.O. Hummel, Infrared Analysis of Polymers, Resins and Additives: An Atlas, Wiley-Interscience, New York, Vol. 1, 1971.
[21] S. Ege, Organic Chemistry, D.C. Heath, Lexington, MA, 2nd edn.,1989, Chap. 10.
[22] C.J. Pouchert, The Aldrich Library of FT-IR Spectra, 1 edn., Vol. 3, Aldrich, 1989.
[23] H. Budzikiewicz, Interpretation of Mass Spectra of Organic Compounds, Holden-Day, San Francisco, CA, 1965, Chap. 6.
[24] R.M. Silverstein, G.C. Bassler, T.C. Morris, Spectroscopic Identification of Organic Compounds, 5th edn., Wiley, New York, 1991, Chap. 2.
[25] Y. Tsuchiya, K. Sumi, J. Polym. Sci., Part A-1 7 (1969) 1599.
[26] A. Holmstrom, E.M. Sorvik, J. Appl. Polym. Sci. 18 (1974) 761.
[27] H. Pines, The Chemistry of Catalytic Hydrocarbon Conversions, Academic Press, New York, 1981, Chap. 1.VI.